In Situ Studies of Phase Stability and Microstructure Evolution in Metal Alloys Under Ion Irradiation in the IVEM at ANL

D. Kaoumi[1]*, A T Motta[1], R C Birtcher[2], M Kirk[2], and P. Baldo[2]

[1] Mechanical and Nuclear Engineering Department, 18 Reber Bldg,

The Pennsylvania State University, University Park, PA, 16802, USA

[2] Materials Science Division, Bldg 212 Argonne National Laboratory, IL 60540 USA

*E-mail: kaoumi@psu.edu

Abstract: One of the difficulties of studying irradiation-induced processes such as grain-growth and second-phase stability is the lack of kinetics information since usually samples are examined ex-situ i.e. after irradiation has been performed, so that only "snapshots" of the process are available. Given the dynamic nature of the phenomena, in situ observation is very useful for better understanding the mechanisms and determining the kinetics of the processes involved. This can be done using the Intermediate Voltage Electron Microscope (IVEM) facility at Argonne National Laboratory and two examples are discussed here. Indeed, grain growth under ion irradiation was studied using free-standing nanocrystalline metallic films. The results showed a temperature-independent regime (under 0.20 Tm), and a thermally-assisted regime where grain-growth increases with irradiation temperature. A model based on thermal spikes was proposed that matches well the observed kinetics. Recent studies include the irradiation stability of precipitates in Oxide Dispersion Strengthened (ODS) steels which is crucial to the performance of these alloys as GenIV reactor components - these alloys are studied in-situ to doses of up to 200 dpa.

1 Introduction

In situ observations in a transmission electron microscope (TEM) were used to study two different aspects of microstructure evolution in metals under irradiation. The

first aspect is grain-growth under ion irradiation which was studied in free-standing Zr, Pt, Cu and Au nanocrystalline thin films under ion-beam irradiation. The second example is the study of the stability of second phase particle dispersions in Oxide Dispersion Strengthened (ODS) steels under irradiation.

2 Irradiation-induced grain growth in nanocrystalline metals

Free-standing Zr, Pt, Cu and Au nanocrystalline thin films were irradiated in-situ in the Intermediate Voltage Electron Microscope (IVEM) at Argonne National Laboratory with Ar and Kr ions to fluences in excess of 10^{16} ion/cm^2. The main experimental results previously reported in [1, 2, 3] are summarized below.

2.1 Summary of Experimental Results

a. Grain growth under irradiation occurs at all temperatures studied. All samples studied showed a gradual increase in the grain size with ion dose at all temperatures, even at temperatures down to 20 K. Figure 1 shows a bright field sequence of the evolution of thin films of Au, Pt and Cu at various fluences when irradiated at room temperature. It is clear that grain growth occurs and that it varies from material to material.

b. Similarly to ion beam mixing phenomena, ion-irradiation induced grain growth exhibits two regimes with respect to irradiating temperature: (i) a low temperature (or "non-thermal") regime in which irradiation effects dominate the grain growth process, and (ii) a thermally-assisted regime where thermal motion and irradiation effects combine to increase the rate of grain growth caused by either of these mechanisms operating alone. The transition temperature between the non-thermal and thermally assisted regimes depends on the material but can be scaled with its melting temperature, occurring at a homologous temperature between 0.15 and 0.20 T_m.

c. The average grain size follows an exponential law with fluence with n ~3: **g**rain-size was measured from the micrographs and plotted versus ion dose. Details about the grain size measurements and the grain growth curve fittings are provided in [2,3]. The grain growth curves revealed a common trend for all compositions considered and for all irradiating temperatures. The ion-irradiation induced grain growth curves could be fitted with the expression: $D^n - D_0^n = K(\Phi t)$ where D_0 is the initial mean grain diameter, Φ is the ion flux, t is the exposure time, n and K are the fitting parameters which varied depending on the material, the temperature. Values of n between 2.5 and 3.5 (average value of 3) were found, revealing a slower grain growth than that predicted by Hillert's model of thermal grain growth driven by grain curvature in conventional polycrystalline materials, for which n=2 [9].

d. Grain-growth did not occur under 1 MeV electron irradiation up to high doses: electron irradiation of Zr based thin-films to doses in excess of 100 dpa showed no increase in grain size. We interpret this result to mean that atomic displacement cascades are needed for grain-growth to occur. This indicates that only defects created within dense subcascades (i.e. thermal spikes) influence grain-growth kinetics.

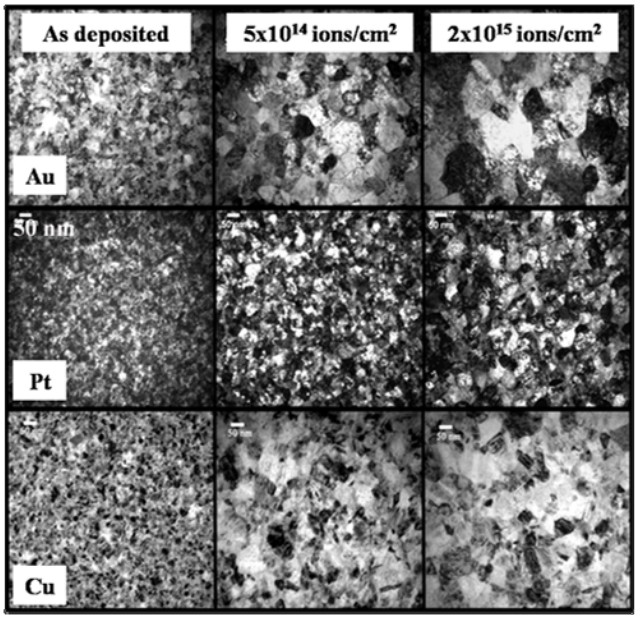

Figure 1: Sequence of bright-field TEM images taken at different ion doses showing grain growth induced by ion-irradiation (from left to right: as deposited, $5x10^{14}$ ions/cm^2, $2x10^{15}$ ions/cm^2). From top to bottom: pure Au and Pt thin-films both irradiated with 500 keV Ar ions and Cu thin film irradiated with 500 keV Kr ions at room temperature.

To account for the experimental observations above, a model for grain growth under irradiation in the "temperature-independent regime" was proposed, based on the presence of thermal spikes.

2.2 Thermal Spike Model of Grain-growth Under Irradiation

2.2.1 Driving force and mechanism for grain-boundary migration

Under thermal conditions, grain growth is considered to happen by grain-boundary migration which is driven by the grain-boundary curvature. The atomic jumps across the grain boundary being biased in favor of reducing the grain-boundary curvature and result in the growth of some grains at the expense of others. Ion-irradiation-induced grain-growth is subject to the same driving force as thermal grain-growth, but the atomic transport mechanisms are different. The picture behind the thermal spike model of ion-irradiation induced grain growth is as follows. As ions interact with matter, primary knock-on atoms are displaced from their lattice sites with some kinetic energy. The PKAs (of high enough energy) subsequently dissipate their energy through displacement (sub)cascades which result in local thermal spikes. Some of these spikes occur within the bulk of grains, others hit near grain-boundaries. When a thermal spike occurs at a grain-boundary it can cause atoms in the thermal spike region to jump across the boundary. These atomic jumps are biased by the local curvature of the grain-boundary (i.e. the local driving force for grain-

boundary migration) such that a net number of jumps across the grain-boundary occur in the direction reducing the curvature, resulting in grain-boundary migration and grain-growth. Two important assumptions underlie the model proposed to describe grain-growth under ion-irradiation in the low-temperature regime.
The first assumption is that only defects created in the direct vicinity of grain-boundaries contribute to grain growth. This assumption is supported by the observation that grain-growth does not depend on substrate temperature in this regime, which implies that long-range thermal diffusion is not significant. At these temperatures the diffusion length is shorter than the recombination radius, supporting the idea that only defects created in the direct vicinity of the grain boundary participate in grain-growth.
The second assumption is that displacements resulting from isolated elastic collisions do not contribute to grain growth. This assumption stems from the observation that no grain-growth was observed during 1 MeV-electron irradiation of the Zr-Fe thin films at room temperature to 80 dpa under electron irradiation whereas in the case of ion irradiation for a similar dose (in terms of dpa), grain-growth clearly occurred in the irradiated area. The main difference between the two types of irradiation is that in the case of electron irradiation, the displacements are homogeneously created, without cascades and therefore without thermal spikes. This shows that there is a need for displacement cascades for grain-growth to occur.

In summary, *in the low-temperature regime, ion-irradiation grain growth is caused by the thermal spikes intersecting grain-boundaries.*

1.2.2 Derivation of the grain-growth rate equation
Based on this picture of the grain-boundary migration, an analytical model was derived to account for the grain-growth kinetics of the *average grain* assumed to be spherical. The details of the derivation can be found in [4]. Eqn 1 gives the fundamental equation determining the kinetics of ion-irradiation-induced grain-growth in the temperature-independent regime as described by the model:

$$\frac{dD}{dt} = \delta \Phi \chi f_{GB} \eta V_{at} \qquad (1)$$

where Φ is the ion flux (taken as constant), χ is the average number of thermal spikes triggered by one ion per unit depth in the thin-film, f_{GB} is the fraction of spikes intersecting the grain-boundary, $\delta/2$ is the width in the grain associated with the grain-boundary, within which the spikes participate in the grain-boundary migration, η is the integrated number of atomic jumps over the lifetime of a thermal spike occurring at the grain boundary (under the influence of the local grain-boundary curvature), and V_{at} is the atomic volume.
The fraction of spikes intersecting grain-boundaries f_{GB} is defined as the fraction of atomic sites close enough to the grain-boundary such that if a thermal spike is induced locally it intersects the grain-boundary and is derived from geometrical considerations. Assuming a spherical shape for the average grain and spike, f_{GB} is the fraction of sites within a distance equal to the spike radius from the grain-boundary:

$$f_{GB} = \frac{3d_{spike}}{D} \qquad (2)$$

where d_{spike} is the size of the average thermal spike.
The determination of the number of jumps (η) induced in a thermal-spike of energy Q is based on Vineyard's analysis of thermal spikes and activated processes [5]. This analysis is based on the assumption that energy is deposited in a very small region, producing a localized increase of temperature which spreads and cools according to the laws of classical heat conduction in a homogeneous continuum. If an activated process (e.g. migration of atoms) is energized by the spike, then the number of elementary steps (e.g. atomic jumps) caused by one spike can be expressed as an integral over space and the cascade lifetime time of the atomic jump rate in the spike. We consider the thermal spike occuring at a grain boundary where the atomic jumps within the spikes are biased by the local driving force due to the grain-boundary curvature. The net rate of atomic jumps across the grain-boundary between R(r,t) is obtained by accounting for the temperature distribution within the spike T(r,t) obtained from solving the heat transfer equation in the volume of the spike. Then we incorporate the driving force in the expression of R(r,t) and integrate over the lifetime and volume of the thermal spike; η is evaluated as:

$$\eta = \frac{4\gamma\nu}{Dk_B}\frac{\sqrt{\frac{3}{5}}\Gamma\left(\frac{8}{3}\right)k_B^{8/3}}{10\pi C_0^{2/3}\kappa_0}\frac{Q^{5/3}}{E_a^{8/3}} \qquad (3)$$

where γ is the grain-boundary surface energy, ν the Debye frequency, Q the energy of the average thermal spike, C_0 the thermal capacity of the material, κ_0 the thermal conductivity, E_a the activation energy for atomic jumps in the spike, k_B Boltzmann constant, Γ is the gamma function.

2.2.2 The grain-growth equation
Finally, by incorporating Eqn 2 and Eqn 3 into Eqn 1, the grain-growth rate becomes:

$$\frac{dD}{dt} = \frac{\Phi\chi\delta}{N_{at}}\frac{3d_{spike}}{D}\left[\frac{4\gamma V_{at}N_{at}\nu}{Dk_B}\frac{\sqrt{\frac{3}{5}}\Gamma\left(\frac{8}{3}\right)k_B^{8/3}}{10\pi C_0^{2/3}\kappa_0}\frac{Q^{5/3}}{E_a^{8/3}}\right] \qquad (4)$$

Eqn 4 relates the time-evolution of the average grain-size with material properties (such as the specific heat, the thermal conductivity, the atomic volume, the Debye frequency, the grain-boundary energy, and the cohesive energy which E_a depends on) with irradiation parameters (such as the ion flux, the average energy, size and number of thermal spikes induced by the ions). It can thus rationalize the differences in grain-growth kinetics observed in materials with similar collisional properties. Finally, after integration, the grain-growth equation for the thermal spike model is:

$$D^3 - D_0^3 = \left[36\gamma d_{spikes}\chi\delta\frac{V_{at}\nu\sqrt{\frac{3}{5}}\Gamma\left(\frac{8}{3}\right)k_B^{5/3}}{10\pi C_0^{2/3}\kappa_0}\frac{Q^{5/3}}{E_a^{8/3}}\right]\Phi t = K\Phi t \qquad (5)$$

Eqn 5 is of the form of $D^n - D_0^n = K\Phi t$ to which the grain-growth curves were fitted. The exponent value of 3 that comes out naturally from the derivation of Eqn 5 is in very good agreement with experimental results, since the fitting of the grain-growth curves showed exponents close to 3 [4]. In the studies by Atwater [6], Liu [7] and by Alexander [8] the exponents were also averaging 3. However this was interpreted as a deviation - due to impurities or internal stresses - from parabolic kinetics (similar to the kinetics given by Hillert's model of thermal grain growth in polycrystalline materials [9]). The present study suggests that this is an *inherent* feature of grain-growth under ion irradiation at low temperatures so that the expected value for the exponent n is 3. The cubic exponent originates from the introduction of the probability term f_{GB}. Although previous studies agreed on the idea that only atomic displacements created at the grain-boundaries participate in their migration and hence in grain-growth [6, 7, 8] no such correcting term was introduced.

3 Phase Stability Under Irradiation of Precipitates in Oxide-Dispersion-Strengthened (ODS) Steels Relevant for the GenIV Nuclear Reactors

This study is an ongoing study. The overall objective is to investigate the phase stability of oxide precipitates in ODS steels under ion irradiation. This information can be used to determine whether the favorable mechanical properties of these steels are maintained under irradiation, thus addressing one of the main materials research issues for this class of steels which are considered as candidates for cladding or structural application in GenIV fast breeder reactors and fusion projects. This research program is closely related to the fundamental understanding of the irradiation precipitation/dissolution problem.

Several alloys have been selected for study among the many ODS steels including MA-957(Fe - 14Cr - 1Ti – 0.3Mo – $0.25Y_2O_3$) and alloy DY (Fe-13Cr-1.5Mo-$1TiO_2$-$0.5Y_2O_3$) both obtained from the CEA (Saclay, France). These alloys exhibit a range of composition and heat treatment and a corresponding range of second phases present. We report here a few results on the DY and MA957 ODS alloys. These ODS alloys follow similar processing methods. For instance, DY alloy is fabricated as following. After the powders are mechanically alloyed in a vibrating ball-mill, they are cold-pressed, and then hot-isostatic-pressed at high temperature (950°C). The extrusion in form of tubes is done at 1150°C with a glass lubricant (the intermediary thermo-mechanical treatment being proprietary). Yttria is added to prevent recrystallization by blocking the dislocation migration. The advantage of using yttria instead of other oxides, carbides, or nitrides is its relative stability at high temperatures. However studies agree on the fact that Y_2O_3 particles initially introduced as powders dissolve during the mechanical milling stage [10] and reform as clusters of Ti-Y-O nano-cluster compounds during the HIP stage. Detailed information about the crystal structure (lattice parameters etc), oxide/matrix interfacial coherency and the formation mechanism of complex oxide particles has not been demonstrated yet.

3.1 In-Situ Ion irradiation of the ODS steels

Ion irradiations were conducted at the Intermediate Voltage Electron Microscope (IVEM)-TANDEM facility at Argonne National Laboratory. Samples were irradiated with 300keV Fe ions at 300 K and 1 MeV Kr ions at 773 K.

3.1.1 300 keV Fe ion irradiation of DY and MA957 alloys at 25˚C

The DY sample was irradiated in situ in the IVEM at 25˚C to $2.5x10^{15}$ ions/cm^2 (~15 dpa). Fig. 2 (left) shows bright field micrograph of the irradiated microstructure after an intermediate ion dose of ~6 dpa. Some of the particles undergo amorphization while others are still crystalline after irradiation, others show a "halo" or "shell" around the edge. This difference in behavior may come from the difference in chemical composition. It is noted that amorphization was not observed in the neutron irradiations (435 to 580ºC) of the same alloy [11]. This difference may be due to the difference in dose rate between ion and neutron irradiations. Amorphization may be possible with neutrons at lower temperatures since there is usually a shift in temperature range between ion and neutron irradiations due to the difference in dose rate (as is the case for void swelling).

The small-size particle population (2nm-5nm) is more difficult to observe under irradiation than the coarser particles (which can reach a few hundred nanometers in diameter) because of the complex contrast stemming from the irradiation damage. Indeed, at 25ºC, irradiation damage does not anneal as fast as higher temperature hence there is more visible damage structure than at higher temperature (in terms of "black dot damage", loops etc). During neutron irradiation (435 to 580ºC), it was reported that the small size oxides disappeared at high doses (~200 dpa) [11]. Also in the neutron irradiations, the big precipitates which dissolved were surrounded by a "halo" of small precipitates. It was suggested that the phenomenon of re-precipitation might have happened after the irradiation was stopped while the DY tube was still in the reactor cooling down; indeed the alloy stayed in the reactor for about 600 hours and therefore spent an equivalent 600 h at 400ºC. If it is the case, re-precipitation is not expected to occur under ion irradiation even for high temperature irradiations because the cooling rate after the irradiation is complete is very fast and would be equivalent to quenching the material.

In the case of MA957 irradiated at 300 K, only some particles have a halo as seen in Fig 2 (right). Chemical composition differences may account for the differences in how particles behave under irradiation. Overall, the particles are more stable with respect to amorphization in this MA957 steel, relatively to DY. It could be that in the case of DY the particles which are more sensitive to amorphization are the carbides or intermetallics. More analysis including EFTEM is ongoing.

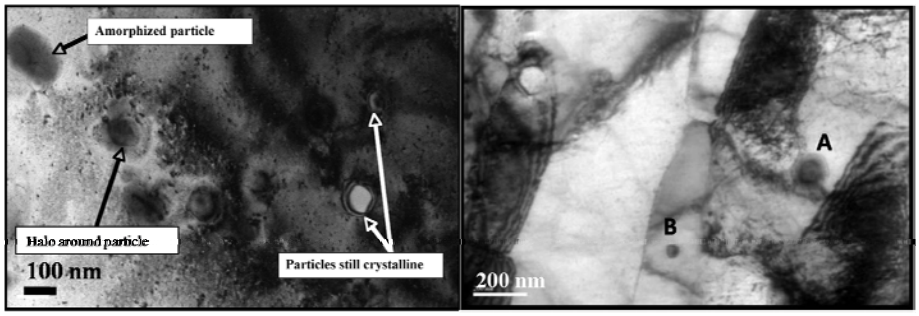

Figure 2: Bright Field micrograph showing effects of 300 keV Fe ion irradiation at 25˚C on (left) DY alloy to a dose of about 10^{15} ions/cm^2 (~6dpa), and (right): MA957 irradiated to $3x10^{15}$ ions/cm^2 (~18 dpa) some particles remain unchanged, others remain crystalline but show a halo at the interface and others are completely amorphized (in DY only).

3.1.1 1-MeV Kr ion irradiation of MA957 at 500˚C:

Fig 3 shows a BF sequence of the same region (at different magnifications) of a MA957 sample irradiated at 500°C to 100 dpa (left) and 200 dpa (right). A qualitative observation is that the grain structure, including sharp grain boundaries, is insensitive to this high level of damage. Also, the dislocation networks that form within the grains appears substantially unchanged from 100 to 200 dpa in the in-situ ion irradiation images. It should be pointed out that the sample tilts are slightly different and thus images of the defect structure vary between the different grains due to changes in diffraction condition with tilt. As far as the dispersion, the bigger particles appear to be more stable than at 25˚Cwith respect to amorphization and surface degradation as can be seen in Fig 3 while the smaller particles (2-5nm) are still difficult to follow. EFTEM would most likely be helpful to follow this population of particles as well as for the determination of their nature. Unfortunately, this cannot be done in-situ at the IVEM and therefore post-mortem investigations are necessary.

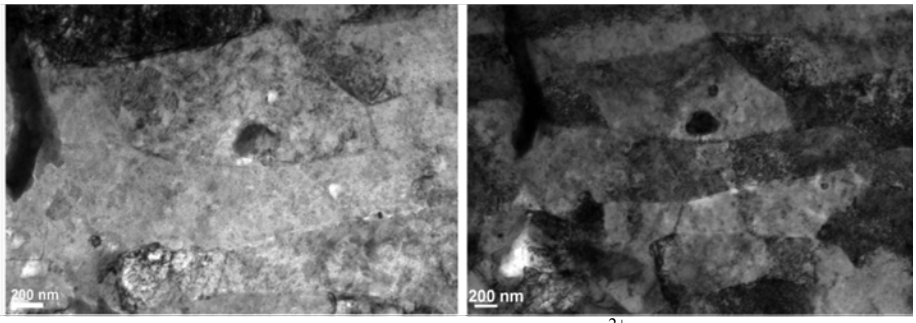

Figure 3: MA957 ODS irradiated in situ with 1 MeV Kr^{2+} to 200 dpa at 500 C: (left) ~100 dpa; (right): ~200 dpa. The grain morphology appears to be very stable (sharp grain boundaries) even at ~200 dpa; the particles followed under irradiation appear to be stable too at this irradiating temperature.

4 Conclusions:

In-situ ion irradiation in the electron microscope is very useful for helping determine the kinetics and mechanisms of irradiation induced processes. This is demonstrated in this paper by two separate studies, on grain growth and precipitate stability under irradiation. In the case of grain-growth under ion irradiation, the in-situ observations allowed to derive a model of the phenomenon based on the direct impact of irradiation-induced thermal spikes on grain-boundaries. The model describes grain growth driven solely by the reduction of grain boundary area. Grain-boundary migration occurs by atomic jumps within the thermal spike biased by the grain-boundary curvature driving force. The model yields a power law expression relating the average grain-size with the ion dose, with an inherent exponent of 3 in good agreement with experiments. The study of the irradiation phase-stability of the dispersion in Oxide-Dispersion-Strengthened (ODS) Steels is an ongoing study. Preliminary results have shown an effect of temperature and chemical composition on the response of the alloy to irradiation. The dispersion appears to be more stable at 500°C than 25°. EFTEM will be useful to determine the effect of the chemical composition with more precision.

Acknowledgements

The experimental part of this research was conducted in the IVEM-Accelerator facility at Argonne National Laboratory, which is supported as a User Facility by the U.S. Department of Energy, Basic Energy Sciences, under contract W-31-109-ENG-38. The expert help of P. Baldo, L. Funk, A. Liu, A. McCormick and E. Ryan was essential to the completion of the experimental part of this work. This study was funded by DOE Nuclear Engineering Education Research program.

References

[1] D. Kaoumi, A. T. Motta, and R. C. Birtcher, *J ASTM International* **4** 8 (2007)
[2] D. Kaoumi, A. T. Motta, and R. C. Birtcher, *Nucl Instrum Methods Phys Res B* **242** (2005) p490
[3] D. Kaoumi, PhD. Thesis, The Pennsylvania State University (2007)
[4] D. Kaoumi, A. T. Motta, and R. C. Birtcher, *J Appl Phys* (in press)
[5] G. H. Vineyard, *Radiat Eff* **29** (1976) p245
[6] H. A. Atwater, C. V. Thompson, and H. I. Smith, *J Appl Phys* **64** (1988) p2337
[7] J. C. Liu, PhD. Thesis, Cornell University (1989)
[8] D. E. Alexander and G. S. Was, Phys. Rev B **47** (1993) p2983
[9] M. Hillert, Acta Metall. **13** (1965) p227
[10] Y. Decarlan, CEA (Saclay, France) (2008)(unpublished)
[11] I. Monnet, P. Dubuisson, Y. Serruys, M. O. Ruault, O. Kaïtasov, and B. Jouffrey, *J Nuc Mater* **335** (2004) p311